Confirmation of Mg/Ca ratios as palaeothermometers in Atlantic limpet shells

Niklas Hausmann[a,*], Donna Surge[b], Ivan Briz i Godino[c]

[a] *Leibniz Zentrum für Archäologie, Ludwig-Lindenschmit-Forum 1, Mainz, Germany, 55116*

[b] *University of North Carolina, 104 South Road, 225 Geology Building, Chapel Hill, NC, US, 27599-3315*

[c] *CONICET-CADIC, AV. B. Houssay, 200., Ushuaia, Argentina, 9410*

Abstract

This study provides a reassessment of magnesium to calcium (Mg/Ca) ratios in Atlantic limpet shells to determine past sea surface temperatures (SST). While *Patella depressa* along the Spanish shoreline and *Patella caerulea* in the Mediterranean have repeatedly produced reliable correlations between SST and Mg/Ca ratios, this relationship is not the case for other patelloid species. Particularly, *Patella vulgata* but also *Nacella deaurata* have been studied using Mg/Ca ratios with mixed or contrary results. In this study, we present elemental maps of these two species as well as *Nacella magellanica* together with oxygen isotope ratios (δ^{18}O) that confirm a good relationship with SST. Our dataset also reassesses a specimen which was previously unsuccessful in providing significant correlations between δ^{18}O values and Mg/Ca ratios. By reassessing these species and including modern and archaeological specimens (n=12) from three patelloid species (*P. vulgata*, *N. deaurata*, and *N. magellanica*) we further add to the growing set of evidence for the reliable use of Mg/Ca ratios to detect palaeotemperature change. As a result, these species can in the future serve to determine ontogenetic age and season of capture as well as to reveal locations of interest within the growth record (i.e. annual temperature minima and maxima) for targeted δ^{18}O and clumped isotope analysis.

Keywords: Sclerochronology, Patella, Nacella, LIBS, Mg/Ca

1. Introduction

Limpet shells are commonly found within archaeological sites and past shorelines due to their robust carbonate structure and the long-term use of limpets as a marine food source (Álvarez et al., 2011, Robson et al. (2023)). They have been successfully studied in the context of coastal subsistence economies and site occupation on seasonal (Shackleton, 1973; Parker et al., 2020; Bosch et al., 2018) or long-term scales (Ortiz et al., 2015), as well as archives of palaeotemperature (Fenger et al., 2007; Surge and Barrett, 2012; Wang et al., 2012; Colonese et al., 2012; Ferguson et al., 2011). Determining past sea surface temperature (SST) change recorded in patelloid limpet shells largely relies on the measurement of δ^{18}O values within the calcitic parts of the shell, but attempts have been made to also use elemental ratios, such as magnesium to calcium (Mg/Ca) ratios (Graniero et al., 2017; Ferguson et al., 2011), to have an alternative measure that potentially provides a more accurate SST estimate than δ^{18}O-values,as the latter proxy is affected by changes in the mixing of fresh- and saltwater. In addition, the data acquisition of elemental ratios

*Corresponding author

Email address: niklas@palaeo.eu (Niklas Hausmann)

— either through laser-ablation-isotope-ratio-mass-spectrometry (LA-ICP-MS) or laser induced breakdown spectroscopy (LIBS), can be much faster and cost-effective, increasing the number of specimens that can be studied overall (Durham et al., 2017; Hausmann et al., 2023).

Problematically, links between Mg/Ca ratios and SST changes in many marine mollusc shells, including limpets, have shown to be unreliable (Surge and Lohmann, 2008; Wanamaker et al., 2008; Schöne et al., 2010; Freitas et al., 2012; Graniero et al., 2017; Poulain et al., 2015; Vihtakari et al., 2017). This is particularly the case where there is little available additional information on metabolic processes, organic components of the shell matrix, intra-increment and intra-shell variability, and growth rates, which can independently and unpredictably affect Mg/Ca ratios and confound their interpretation as a temperature proxy. Confusingly, in some cases multiple different temperature equations have been found for the same species (see Freitas *et al.* (2012) and Vihtakari *et al.* (2017) and references therein). Coeval specimens sharing one locality can also show differences in their relation to SST (Hausmann et al., 2019). Where the use of Mg/Ca ratios as a palaeotemperature proxy was successful, anomalous patterns in some specimens had to be filtered out by hand, reducing the overall robustness of the results of those successful studies (Ferguson et al., 2011).

Recent research particularly of *Patella* spp. in the Mediterranean and southwest Europe have provided promising results (Hausmann et al., 2019; García-Escárzaga et al., 2015, 2018). However, there remains a lack of clarity for Atlantic limpet species, particularly since it was shown, that the Mg/Ca ratio in their shells are not reliable recorders of palaeotemperature (Graniero et al., 2017). Using modern reference material Graniero *et al.* (2017) tested multiple elemental ratios (Mg/Ca, Sr/Ca, Li/Ca, Li/Mg, and Sr/Li) acquired via LA-ICP-MS measurements with no ratios showing correlations with corresponding SST changes nor any sinusoidal patterns that would indicate a seasonal environmental control of elemental ratios. This study included two species also used in our study (*Patella vulgata*, *Nacella deaurata*), with one *P. vulgata* specimen (i.e. specimen ORK-LT5) being analysed by both. We also added specimens of the species *Nacella magellanica,* which — similar to the other two species — is also an established palaeothermometer using δ^{18}O-values (Colonese et al., 2012; Gutiérrez-Zugasti et al., 2017; Nicastro et al., 2020).

In this study, we repeat and expand upon the analysis of Atlantic limpets to determine the reliability of Mg/Ca ratios as palaeotemperature proxies. To do this, we sampled a set of previously published and unpublished limpet specimens dating to modern and archaeological contexts using LIBS. LIBS allows us to carry out 2D imaging of entire shell sections, which facilitates navigation of the complex elemental structure of the shell and a better separation of the external, temperature-related changes from the internal and less understood factors that influence the Mg/Ca ratio. By working with already published datasets, we were able to simultaneously avoid costs for new high-resolution δ^{18}O-data, to use real-world examples, and to also provide pilot-data for areas of existing research interest. Generally establishing the usefulness and reliability of Mg/Ca ratios as SST proxy in limpets provides a platform for future research and an important steppingstone to a better understanding of elemental ratios in other marine mollusc shells.

2. Materials and Methods

2.1. Limpet specimens

The analysed specimens, their origin and respective studies with research background information can be found in Table 1. Here we will briefly summarise their contextual information, which can be accessed in more detail from the respective studies (Nicastro et al., 2020; Surge and Barrett, 2012; Graniero et al., 2017). While those studies also included other specimens, their accessibility or state of preservation did not allow them to be re-analysed.

Table 1: Overview of the modern and archaeological limpet specimens analysed in this study.

Context	Study	Species	Location	Sample ID	Previous analyses
Modern	(Nicastro et al., 2020)	*N. deaurata* *N. magellanica*	Cambaceres Bay - Tierra del Fuego (AR)	ND-1016-3 ND-1016-4 NM-1016-1 NM-1016-3	δ^{18}O and δ^{13}C analysis
	(Graniero et al., 2017)	*P. vulgata*	Rack Wick Bay - Westray (UK)	ORK-LT5	δ^{18}O and δ^{13}C analysis; Mg, Li, Sr, Ca
Archaeological	(Surge and Barrett, 2012)	*P. vulgata*	Rack Wick Bay - Westray (UK)	QG1-7188-1 QG1-7189-2 QG2-1061-1 QG2-1064-1 QG2-7180-1 QG2-7180-2 QG1-7246-1	δ^{18}O and δ^{13}C analysis

Specimens were sourced from two main locations: the Beagle Channel in Tierra del Fuego (Argentina) and the island of Westray in the Orkney archipelago of Scotland (UK). Four modern specimens were collected from the Beagle Channel in Cambaceres Bay in October 2016. The area receives around 570 mm of annual precipitation, but the channel waters are predominantly influenced by marine currents and in the period of October 2015 to October 2016 stayed around 30.7 ± 0.7 psu (practical salinity units) (Nicastro et al., 2020). SSTs range from 30.5ºC in August to 31.9ºC in February (Figure 1 – red line).

On Westray one modern shell (ORK-LT5) was collected in Rack Wick Bay in August 2009 and has been previously analysed for δ^{18}O and δ^{13}C values, as well as for elemental ratios via LA-ICP-MS (Graniero et al., 2017). Westray lies about 70 km north of the Scottish mainland and experiences virtually no freshwater input with salinity values of 34.0 – 34.5 psu (Inall et al., 2009). The annual SST ranges from 34.4ºC in March to 35.3ºC in August (Figure 1 – blue line).

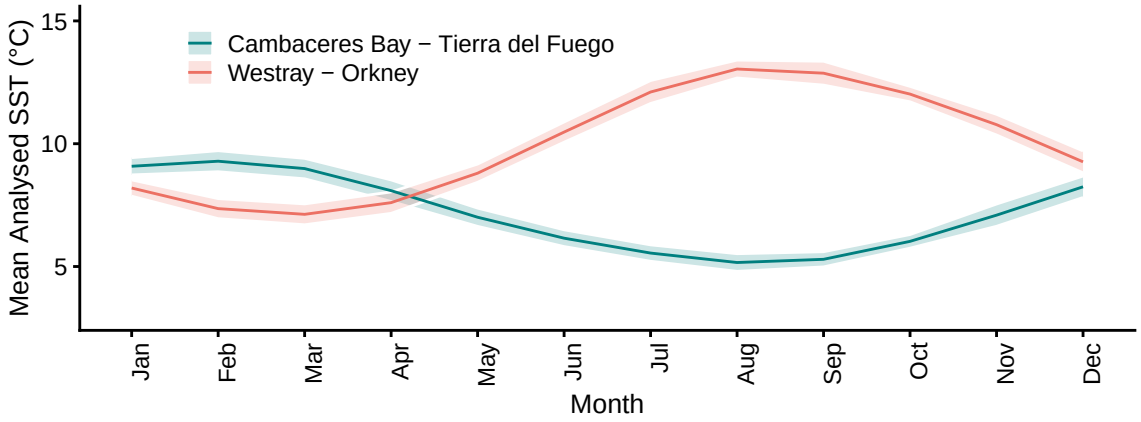

Figure 1: Monthly sea surface temperature values averaged from 2007 to 2023. Values were sourced from Good et al. (2020).

We also studied 7 archaeological specimens of *P. vulgata* from the Quoygrew site on Westray dating to 900 – 1200 CE. These shells have previously been studied to characterise seasonal temperature change during the Medieval Climate Anomaly (810 – 1229 CE) (Surge and Barrett, 2012).

2.2. Methods

2.2.1. Oxygen isotope ratios

High-quality δ^{18}O values were acquired from previous publications on *P. vulgata* (Surge and Barrett, 2012; Graniero et al., 2017), *N. deaurata* and *N. magellanica* (Nicastro et al., 2020), in which detailed descriptions of the methodology for the stable isotope analyses can be found. In short, all shells were sectioned along the maximum growth axis to expose the internal growth structure. From the exposed section carbonate powder samples were acquired using a micromill with resolutions of 100–200 µm and by targeting the calcitic layers of the shells (m+2 and m+3, see (Fenger et al., 2007)). The exact location of the sampled carbonate powder is not available apart from the distance to the growth edge, where reported. Analytical precision of the isotope ratios was consistently at 0.05–0.10‰ and values are reported in per mil units (‰) relative to the VPDB (Vienna Pee Dee Belemnite) standard.

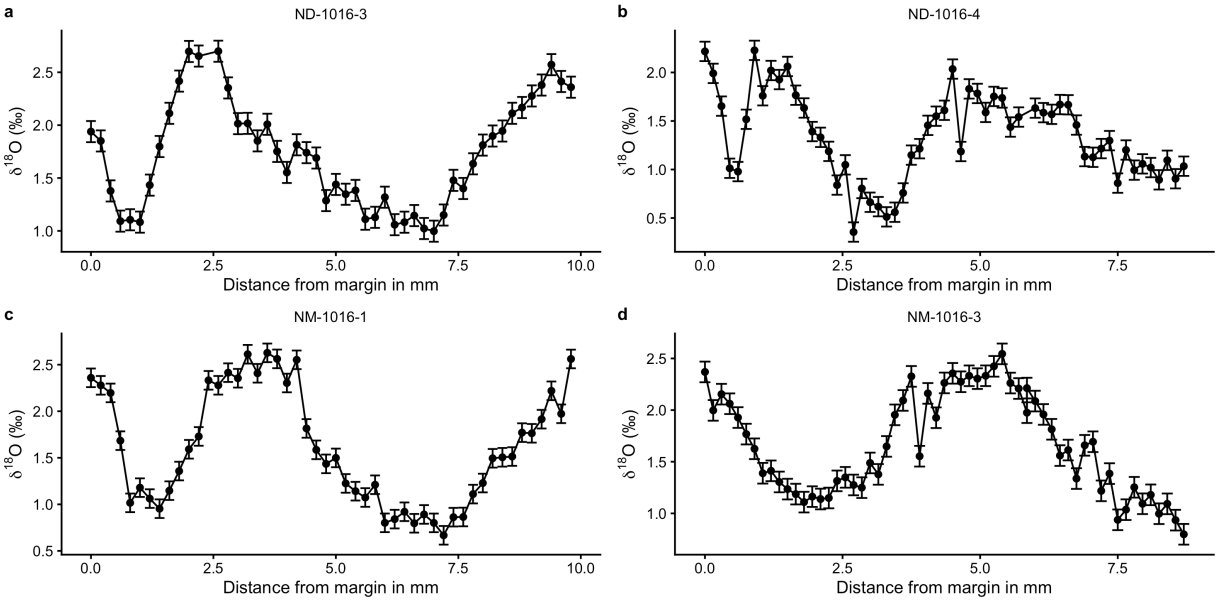

Figure 2: Isotope values of *Nacella* spp. limpet shells from Cambaceres Bay.

Figure 2 and Figure 3 show the previously acquired sequential δ^{18}O-values of limpet shells by species (*Nacella* spp., and *Patella vulgata*, respectively). Due to the high-resolution sampling, all shells show seasonally resolved and multi-year quasi-sinusoidal records of SST change, with *Nacella* spp. shells living 2–3 years and *P. vulgata* living regularly over 3 years. In those instances where longer lifespans resulted in slow growth rates below 1 mm/yr (i.e. specimen QG1-7246-1, Figure 3 b), the temporal-resolution is reduced from more than a dozen of samples per year, to only around 7. Together they show a range of lifespans, with some comparatively long lived for their size (QG1-7246-1, 12 years within 16 mm of growth) making them particularly susceptible to within-shell time-averaging because of slow growth rates. That said, the majority yielded sufficiently fast growth to nearly capture seasonal amplitudes of SST with ages of 2–3 years (n=3), 3–4 years (n=2), and 5 years (n=2).

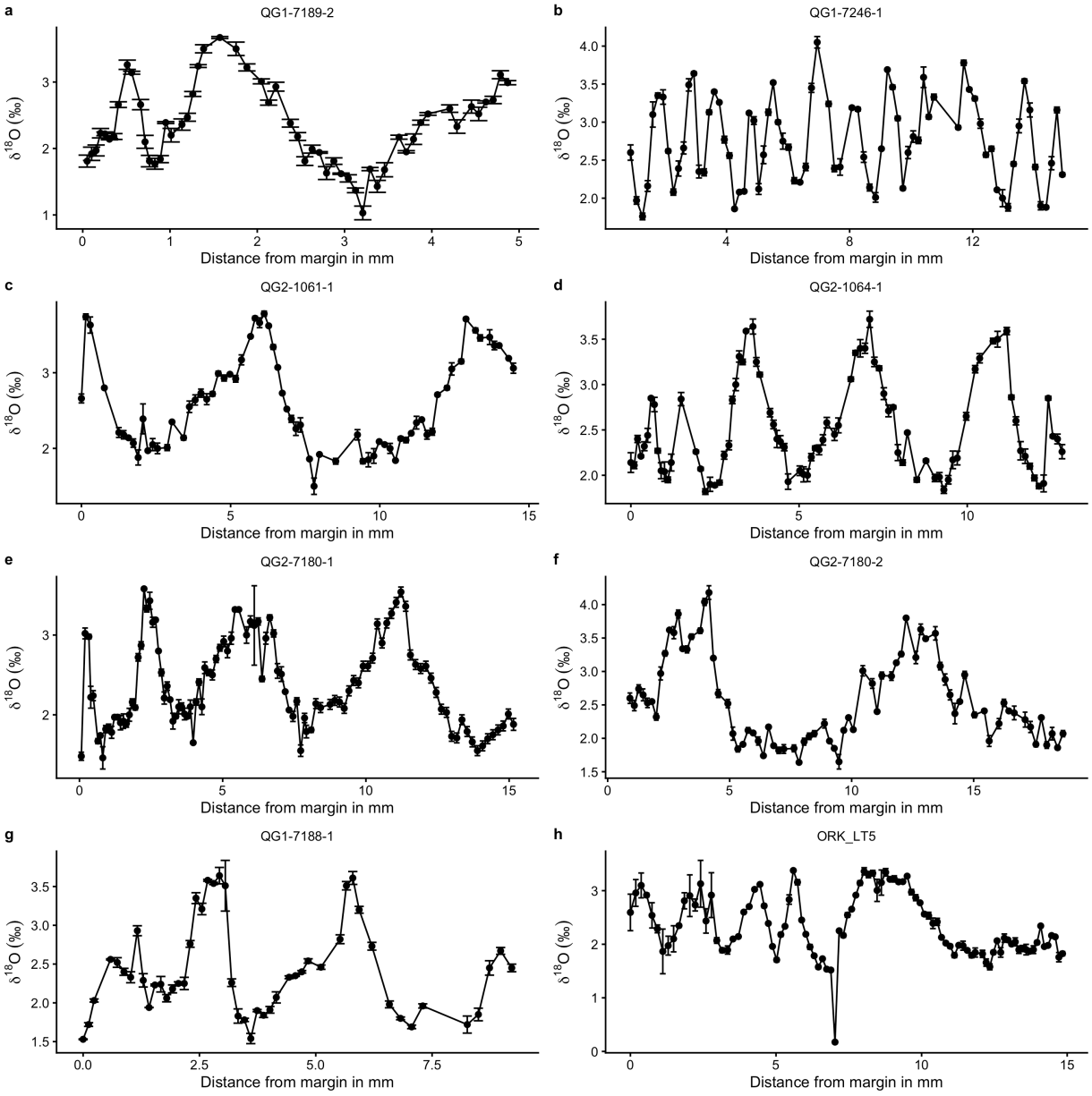

Figure 3: Isotope values of *Patella vulgata* limpet shells from Quoygrew (QG, *a*-*g*) and Rack Wick Bay (ORK, *h*) on Westray, Orkney.

2.2.2. Mg/Ca ratios

Mg/Ca elemental imaging was carried out using LIBS at the Leibniz Zentrum für Archäologie (Mainz-Germany) following previously published methods (Hausmann et al., 2023). The imaging involves the ablation of the shell section using an infrared (1064 nm) laser (1—2 mJ, 100 Hz) onto a surface area of 20—30 µm to generate a plasma plume. This plume emits light, which is measured using a synchronised spectrometer (delay time = 0.5 µs, integration time = 1 µs). The resulting light spectrum quantifies the emission lines of magnesium (MgII: 279.553 nm) and calcium (CaII: 315.887 nm) to determine their intensity ratio. While these two peaks alone do not represent the molar concentrations of both elements (as opposed

to calibration free LIBS; e.g. (Martínez-Minchero et al., 2023)), the intensity ratio is linearly correlated to the molar concentration (Hausmann et al., 2017) and can be used as a reliable indicator of Mg/Ca variation within the shell carbonate. All values reported here are in arbitrary units based on the ratio of intensities of the peaks above.

Using this system we carried out elemental imaging of the shell specimens at a resolution of 50–100 µm distance between sampling spots. Each spot was irradiated 10 times with the first 3 spectra discarded as a cleaning step and the remaining spectra summed to get an average Mg/Ca intensity ratio for each sample spot. Subsequently, we re-sampled the section using a line scan at 10 µm resolution. This leads to an overlap between sample spots, but also allows for a continuous record without gaps. Intensity ratios were filtered for cases with high relative standard deviation (i.e., more than 10%). These occurred in places where the previous sampling procedures for carbonate powder as part of the oxygen isotope analysis left an uneven sample surface introducing variability in the plasma generation and thus uncertainty in the data of these locations.

2.3. Dynamic Time Warping

Because it is not possible to directly associate the exact sample locations used in the analysis of oxygen isotope ratios with the LIBS data, we used dynamic time warping (DTW) to align the time series of $\delta^{18}O$ values and Mg/Ca ratios. DTW is an algorithm that measures similarity between two proxy sequences, which may vary in sampling resolution or interval. By stretching or compressing sections of the series, DTW finds the probable alignment between the two sequences. This allows us to compare the proxy datasets more effectively, ensuring that the temporal dynamics of each shell are accurately matched despite possible discrepancies in sampling intervals or rates. We applied the DTW algorithm using the `dtw` package in R (Giorgino, 2009; R Core Team, 2020), which provides a robust framework for aligning time series data. This can involve selecting appropriate distance measures and constraints to ensure meaningful alignment. We used the default settings for symmetric step patterns and euclidean distance measures (see code in Hausmann et al.(2024)).

3. Results

3.1. Patella vulgata

The elemental imaging of *P. vulgata* shells consistently showed repeating patterns of Mg/Ca intensity ratio changes with high Mg/Ca intensity ratios indicating high temperature periods and low ratios indicating low temperature periods. As examples, Figure 4 shows the 2D-distribution of elemental ratios across the entire section of ORK-LT5 and the preserved anterior side of QG1-7188-1 (additional maps can be found in the supplementaries). The repeating patterns are found across the calcitic layers that are exterior to the myostracum (layers m+2 and m+3) as well as the layers that are interior (m–2)(see Fenger et al. (2007) for a detailed explanations of microstructural layers in *P. vulgata*). The layer m-1, which is also interior, consists of aragonite and is seen in Figure 4 in grey, as its Mg/Ca intensity ratio consistently falls below the range of interest (0.2 and above). Compared to other patelloid shells, some of whose interior is almost entirely made of aragonite, this layer is very thin.

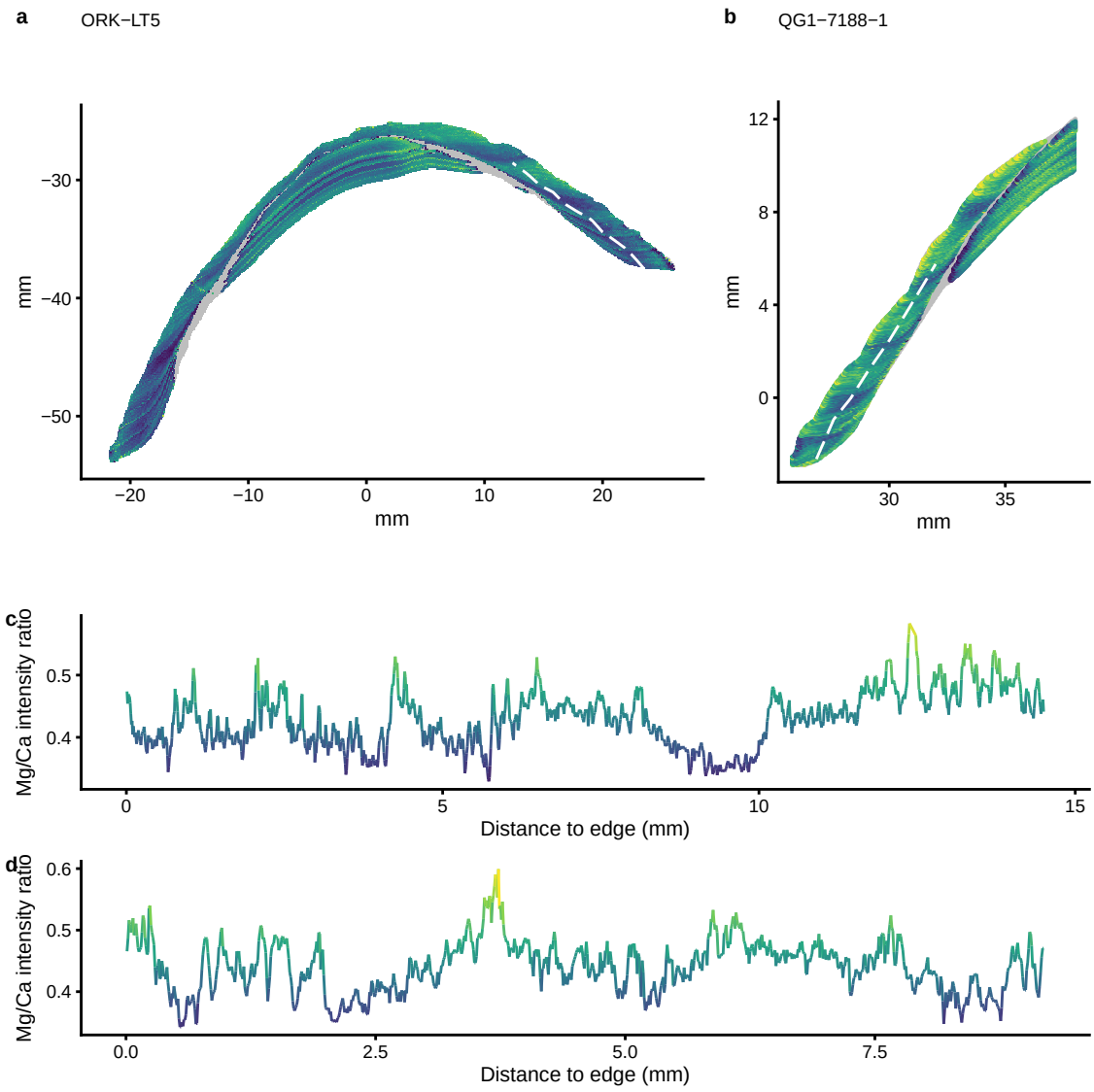

Figure 4: Example LIBS maps and line scans of analysed specimens. (a+c) ORK-LT and (b+d) QG1-7188-1. Note that the ranges of Mg/Ca intensity ratios are not identical but are chosen arbitrarily to increase contrast. Areas in grey consist of low-Mg aragonite and fall outside the chosen colour-range. White dashed lines indicate location of line scans.

Both specimens in Figure 4 show increased Mg/Ca intensity ratios towards the outside of the shell and some degree of intra-increment variability. This is particularly visible in Figure 4 b, where Mg/Ca intensity ratios range from ~0.5–0.7 in the first year of growth (9-–12 mm on the y-axis). A similar pattern is visible in the interior m-2 layer of ORK-LT5 (Figure 4 a), which increase towards the anterior of the shell (0–10 mm on the x-axis).

Line scans also indicate well the quasi-sinusoidal change of Mg/Ca intensity ratios expected based on the stable isotope data and elemental imaging. That said, some of the variability of Mg/Ca intensity ratios within one season such as the summer period of QG1-7188-1 between 0.5 and 2.0 mm distance to the shell edge (Figure 4 d), is visible in a more dramatic manner than it appears in the 2D image. This shows the downside of line-scanning as opposed to the broader milling approach used for the analysis of carbonate

powder (Ferguson et al., 2011).

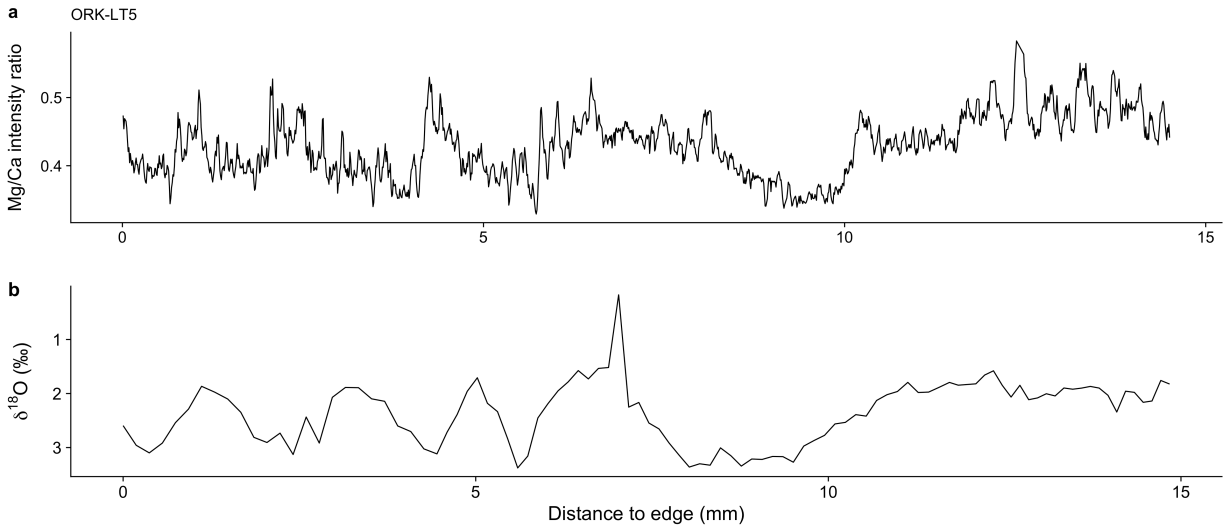

Figure 5: Comparison of LIBS line-scan and sequential δ^{18}O-values of specimen ORK-LT5

Figure 5 shows the line scan of ORK-LT5 in comparison to its δ^{18}O values (similar graphs for other specimen can be found in the supplementaries). The measurements of the distance to the shell edge are not entirely identical, most likely because one growth increment can have a range of distances to the edge, depending on where one measures, and a line scan along the interior would be shorter than a line scan along the exterior. That said, increases and decreases of both proxies seem to mirror each other and to be well aligned.

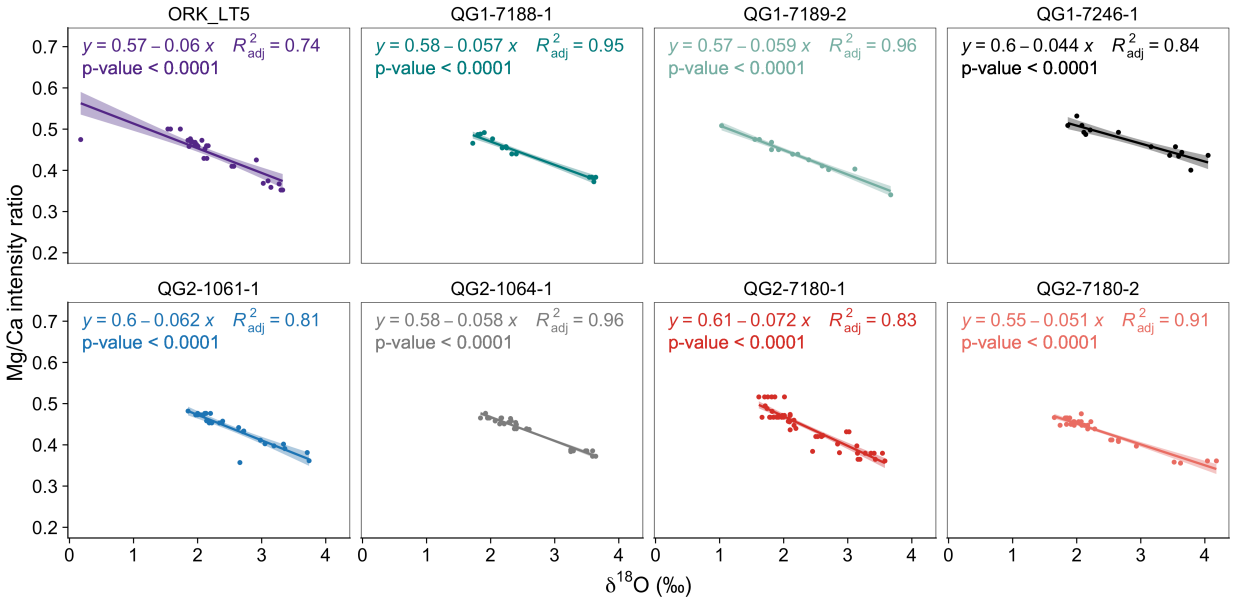

Figure 6: Correlation graphs for Mg/Ca and δ^{18}O values in *P. vulgata* specimens.

Aligning the records programmatically using dynamic time warping, allowed us to compare both proxies

for each specimen directly to determine specimen-specific equations and quantify the correlation of both proxies (Figure 6). The equations for all specimens are different but the majority (barring one: QG1-7246-1) do seem to cluster around shared parameters ($\delta^{18}O = 0.6 - 0.065 * Mg/Ca$). The various coefficients of determination (R^2) range between 0.81 (QG1-7246-1) and 0.95 (QG1-7189-2). These specimens are also the oldest and youngest specimens, respectively, suggesting that lower growth rates and time averaging had a negative effect on the correlation of both proxies. The mean R^2 value of the individual *P. vulgata* specimens is 0.89, suggesting a generally good fit between the two proxies. P-values are overwhelmingly significant and consistently below $p<1e^{-6}$.

3.2. Nacella *spp.*

The LIBS data for *Nacella* spp. specimens is less straightforward with shells being much thinner than *P. vulgata* and thus patterns being more difficult to discern. Both specimens (ND-1016-3 and NM-1016-3) shown as examples in Figure 7 (see additional graphs in supplementaries) also experience increases of Mg/Ca intensity ratio towards the exterior of the shell, similar to the *P. vulgata* specimens from Orkney. This intra-increment heterogeneity combined with the thinness of the shell, further complicates their analysis compared to *P. vulgata* or other *Patella* species (Hausmann et al., 2019). Nevertheless, repeating patterns were visible in the anterior section of the shell, which were also mirrored in the inner layers (m-2) of specimens NM-1016-3 (Figure 7 b).

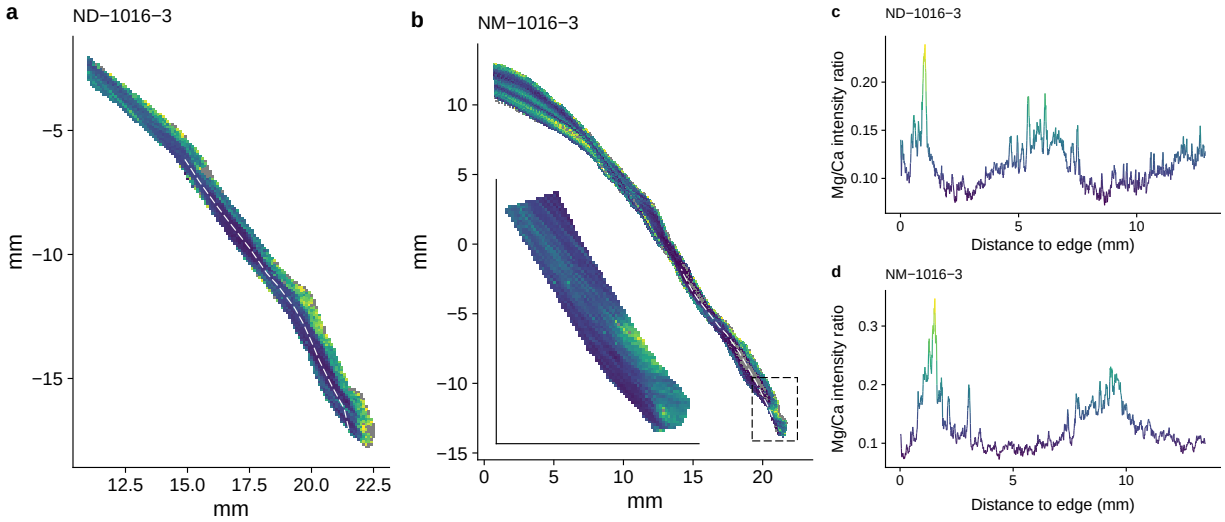

Figure 7: Example LIBS maps and line scans of analysed *Nacella* spp. specimens. (*a*+*c*) ND-1016-3 and (*b*+*d*) NM-1016-3. Note that the ranges of Mg/Ca intensity ratios are not identical but are chosen arbitrarily to increase contrast. Areas in grey consist of low-Mg aragonite and fall outside the chosen colour-range. Note the inset in (*b*) where the shell edge has been resampled using a higher resolution (50 µm instead of 100 µm) to better understand the Mg/Ca ratios at the shell edge. White dashed lines indicate location of line scans.

Interestingly, the Mg/Ca intensity ratios in the *Nacella* spp. shells were much lower (0.05–0.30) than those seen in other patelloid species (e.g. 0.3–0.7 in *P. vulgata* above, or 0.5–1.5 in Hausmann *et al.* (2023)) using the same emission lines. While the intensity ratio depends chiefly on the chosen emission lines to calculate the proportion of the chosen magnesium to the chosen calcium peak, the low ratios still indicate lower concentrations than seen elsewhere or seen only in aragonitic parts of e.g. *Patella* shells. Similar observations have been made before (Graniero et al., 2017). Strong intra-increment heterogeneities are visible along the exterior of the shells (m+3 layer), where Mg/Ca intensity ratios are higher, particularly in specimen ND-1016-3 (Figure 7). The step from lower to higher along the increment is not gradual, as is the

case in NM-1016-3 (see inset of Figure 7 b), but rather stepwise. Sampling across this boundary in a linear scan would most likely lead to erroneous results. Also sampling across gradual changes as in NM-1016-3 can influence the overall correlation graph for a specimen.

Line scans reflect well the changes previously indicated by δ^{18}O values and also indicate about two years of recorded growth. That said, the 2D imaging suggests that in both specimens a third summer can be added to the total record, which is not captured by the line scans.

Figure 8 shows the line scans of ND-1016-3 and NM-1016-3 in comparison to their δ^{18}O values (similar graphs for the other *Nacella* spp. specimens can be found in the supplementaries). Compared to the *P. vulgata* records, these mirror each other much more clearly, due to the brief period recorded in the shells and thus a lower chance of misaligning annual extremes.

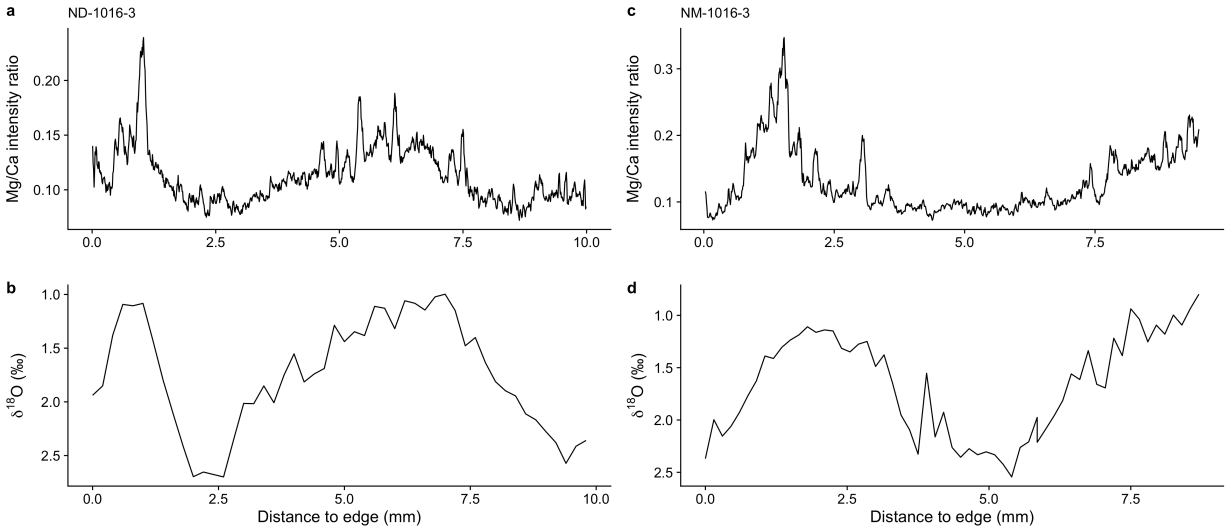

Figure 8: Comparison of LIBS line-scan and sequential δ^{18}O-values of *Nacella* spp. specimens.

The *Nacella* spp. specimens showed similarly clustered correlations, which interestingly were not grouped by species. In fact, specimens ND-1016-3 (*Nacella deaurata)* and NM-1016-3 (*N. magellanica*) are almost identical in their fitted equations (Figure 9). Both also share a high coefficient of determination (R^2) of 0.95 and 0.92 respectively, with the remaining specimens being somewhat lower (R^2 = 0.76 for ND-1016-4 and R^2=0.84 for NM-1016-3). The mean R^2 value for each *N.* species is 0.86 for *N. deaurata* and 0.88 for *N. magellanica* with p-values for all speciemns being far below 0.0001. Why two specimens of different species are so well aligned is not entirely certain and randomness cannot for now be ruled out. That said, since they both have a high R^2 value, it might just be that they were both minimally affected by factors other than SST, including the sampling location of our line scans.

4. Discussion

The Mg/Ca ratios from the 2D elemental imaging present results suggesting that SST is the main factor influencing variations in Mg/Ca ratios in three Atlantic limpet species. Annually repeating patterns of increasing (spring/summer) and decreasing (autum/winter) SST were also visible in the line scans, albeit less straightforward than in the 2D-data. Nevertheless, the resulting mean R^2-values comparing Mg/Ca and ^{18}O values for each species were high (*P. vulgata* R^2=0.89, *N. deaurata* R^2=0.86, *N. magellanica* R^2=0.88). These results are similar to previously published data on other *Patella* species shells (Table 2): R^2 values of *P. depressa* lie between 0.78 and 0.87 (García-Escárzaga et al., 2021), for *P. caerulea* from the Mediterranean

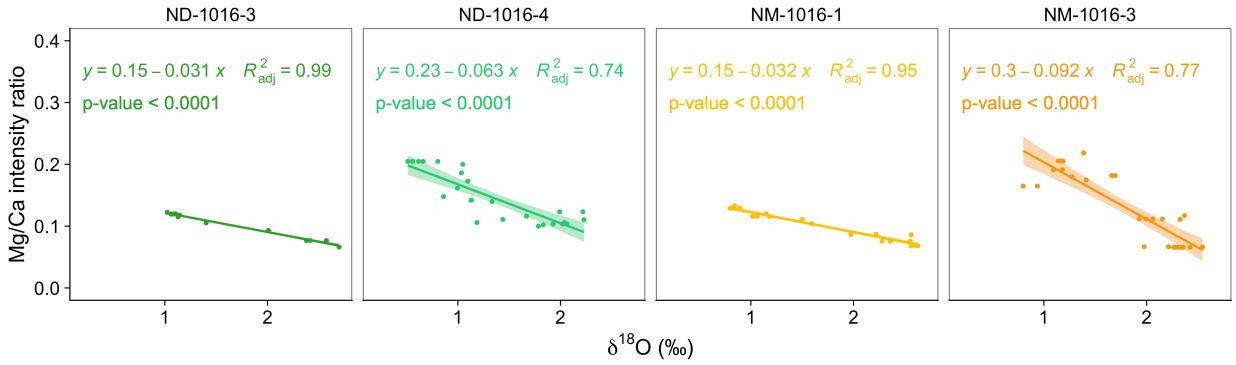

Figure 9: Correlation graphs for Mg/Ca and δ^{18}O values in *Nacella* spp. specimens

between 0.78 and 0.96 — barring one outlier of 0.33 (specimen MP64A), which had increased Mg/Ca ratios in increments with rich organic contents (Hausmann et al., 2019).

Table 2: Correlations of Mg/Ca ratios with δ^{18}O values found in other studies. Bold R^2 values are interpreted as outliers. * indicates samples that were used to determine a shared R^2-value of 0.79.

Species	Locality	Specimen	R^2	Study
P. depressa	Northern Spain	LAN541	0.87	(García-Escárzaga et al., 2021)
		LAN545	0.86	
		LAN554	0.78	
		LAN559	0.82	
P. caerulea	Croatia	ISTPC1	0.9	(Hausmann et al., 2019)
		ISTPC2	0.84	
	Crete	AF1911A	0.91	
		AF3003A	0.92	
	Israel	AKKPC2	0.96	
		AKKPC3	0.89	
		FRMPC1	0.84	
		FRMPC2	0.96	
	Libya	MO31A	0.83	
		MP64A	**0.33**	
		MP67A	0.96	
		MP68A	0.81	
	Malta	MA10	0.82	
	Tunisia	TUNPC1	0.81	
		TUNPC2	0.78	
	Turkey	ANTPC1	0.95	
		ANTPC2	0.93	
		KIZPC1	0.94	
		KIZPC2	0.86	
P. rustica	Gibraltar	**JL1**	**0.02**	(Ferguson et al., 2011)
		JL2	0.8*	
P. caerulea	Gibraltar	JM00	0.69*	
		JM30	0.83*	
P. vulgata	Orkney	ORK-LT5	not reported, here 0.88	(Graniero et al., 2017) and this study
		QG1-7188-1	0.88	this study
		QG1-7189-2	0.95	
		QG1-7246-1	0.81	
		QG2-1061-1	0.90	
		QG2-1064-1	0.90	
		QG2-7180-1	0.87	
		QG2-7180-2	0.90	
N. deaurata	Tierra del Fuego	ND-1016-3	0.95	
		ND-1016-4	0.76	
N. magellanica	Tierra del Fuego	NM-1016-1	0.92	
		NM-1016-3	0.84	

P. rustica has two studied specimens (JL1 and JL2) with R^2-values of 0.02 and 0.80, respectively (Ferguson et al., 2011) (see also Supplementaries). Together with the data from two *P. caerulea* shells (JM00 and JM30 with R^2-values of 0.69 and 0.83), the data from JL2 was used to determine a general Mg/Ca-SST relationship with an R^2 value of 0.79. JL1 was disregarded in that calculation, as well as the second year of growth in JM00, which produced anomalous data. While no additional information about those specimens is available, it seems likely that the discarded Mg/Ca ratios from JM00, which were interpreted as an ontogenetic trend, were potentially influenced by the same intra-increment heterogeneity we see in some of our shell specimens as well. Since these shells were analysed by homogenising the carbonate powder of the m+2 layer and the more exterior m+3 layer, these heterogeneities could have potentially increased the Mg/Ca ratio unpredictably, leading to what might look like an ontogenetic trend in a linear dataset. Whether these anomalies affected JL1 in the same way, albeit stronger, is not clear but it might well be possible. Previous studies of *P. caerulea* found similar patterns of anomalous Mg/Ca values in the m+3 layer (Hausmann et al., 2019). These areas can be avoided using a 2-dimensional approach and if the growth increment is sufficiently wide. These heterogeneities within growth increments are little understood but some research points towards a zonation of the mollusc's mantle and along the growth edge (Lazareth et al., 2013). This zonation could differentially influence the transport of Mg ions to the extrapallial fluid and into the shell.

Another shell whose results we aim to explain further is ORK-LT5 (see Supplementary Information), which has previously been shown to have no substantial correlation with $\delta^{18}O$ values or SST by implication (Graniero et al., 2017). In contrast to other specimens in this study, we were able to resample this specimen and acquire Mg/Ca data on a slightly higher resolution (20–30 µm spots in a 100 µm raster compared to 50 µm spots spaced at 150–300 µm) and using 2 dimensions, as well as using a continuous high-resolution line-scan at (20–30 µm spots spaced at 10 µm) (Figure 10). These additional data revealed previously missed summer peaks at around 2–3 mm distance to the shell edge (grey box in Figure 10) and revealed additional growth at the very edge (dashed box in Figure 10) mirroring the change towards warmer temperatures at the time of collection (August). Including these missing parts lead to a better alignment of both records and a resulting R^2-value of 0.88 (Figure 10).

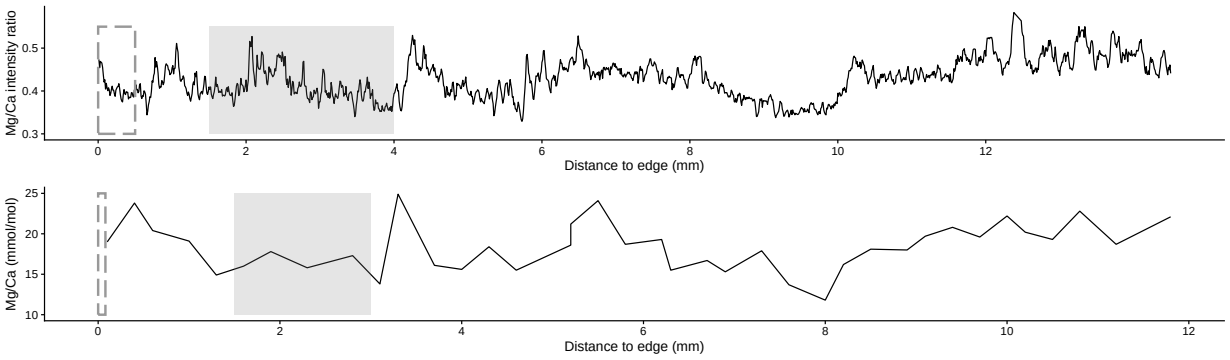

Figure 10: Comparison of previous and new Mg/Ca data for ORK-LT5 explaining the previously unsuccessful correlation of Mg/Ca and $\delta^{18}O$-values.

We were not able to resample the *Nacella* spp. specimens in Graniero *et al.* (2017), which had similarly unrelated records of $\delta^{18}O$ values and Mg/Ca ratios and pointed to no relationship between elemental ratios and SST at all. However, we were able to source other modern specimens of the same species from Tierra del Fuego, which shall serve here as an indicator. Similar to other patelloid shells, the results of the *Nacella* specimens in our study were successful with high R^2 values (0.76–0.95) and suggest Mg/Ca as a reliable proxy for SST (Figure 8 and supplementaries). Why these results are different from the studied *Nacella* spp. specimens in Graniero *et al.* (2017) is not obvious, but the occasional alignment of the Mg/Ca and $\delta^{18}O$ records of their shells (Figure 6 in Graniero *et al.* (2017)) indicate that there is some relationship that — potentially due to the low sampling resolution or intra-increment heterogeneity — is not perfectly visible,

leading to an overall result of an uncorrelated relationship between Mg/Ca ratios and SST.

4.1. Temperature correlation

We further related the Mg/Ca ratios of the modern shells to actual SST data from the respective localities (Figure 1). The data for ORK-LT5 from Orkney were cut to the time period between the start of our available SST data (2007) and the time of collection (August 2009). For the *Nacella* spp. from Cambaceres Bay we chose an overlapping time period, to make the results more comparable between the specimens, which is the lifespan of the youngest specimen NM-1016-3 from January 2015 to October 2016, the time of collection for all 4 specimens.

As indicated by the stable isotope values, no reliable shared relationship between the data can be established, but each shell's Mg/Ca data individually have a good correlation with SST (R^2 values between 0.93 to 0.96 with p-values consistently below 0.001) (Figure 11), which are even better than the correlation between elemental ratios and stable isotope values. This improvement is most likely due to the simple and sinusoidal SST curve, which is easier to fit to other data.

As a result of the different correlations between Mg/Ca ratios and SST in the modern shells, we did not attempt to use Mg/Ca as a direct proxy for absolute SST values in ºC for the archaeological shells from Quoygrew, but rather as a proxy for relative SST change (i.e. warmer/colder). In future analyses, these high resolution and rapidly acquired records of relative SST can guide the sampling for oxygen isotope or clumped isotope analysis and reduce analytical costs per shell, thus increasing the quantity of shells that can be analysed per study.

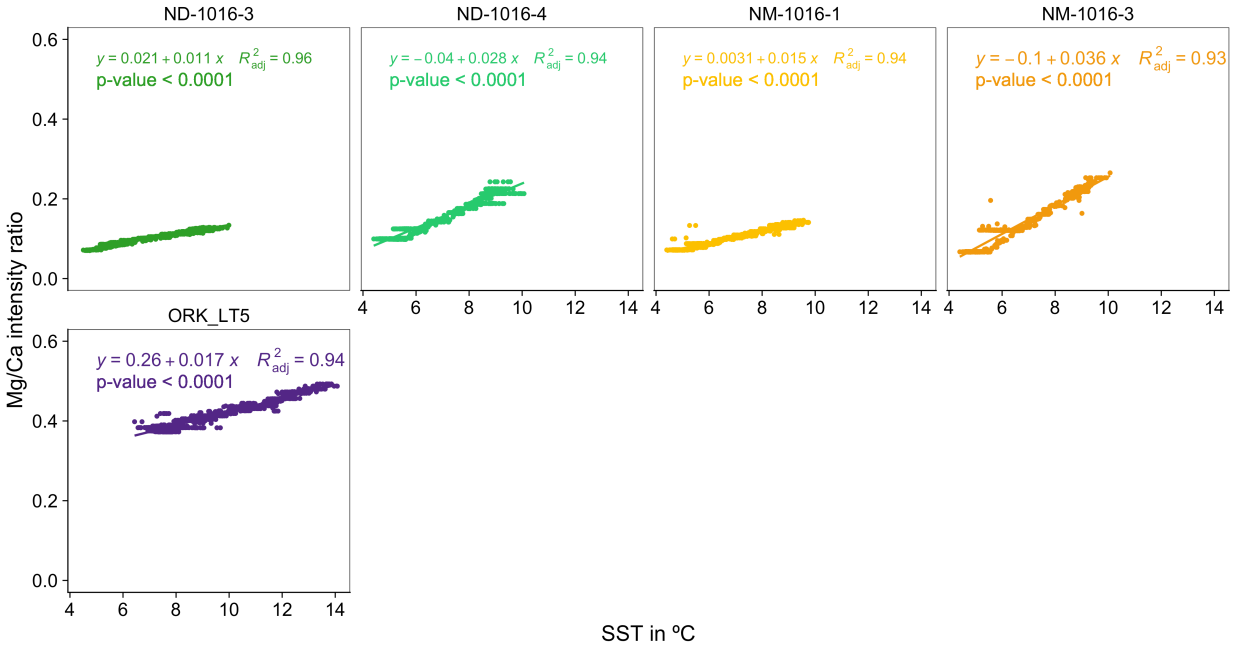

Figure 11: Comparison of Mg/Ca and SST in all modern shells.

5. Conclusion

This study uses LIBS as a novel analytical tool to present high-resolution and 2D information on Mg/Ca concentrations in modern and archaeological patelloid shells and their relationship to sea surface temperature. The results for *P. vulgata*, *N. deaurata*, and *N. magellanica* were consistently promising with mean R^2 values of 0.89, 0.86, and 0.88 respectively.

LIBS elemental imaging provided insight into elemental anomalies found particulary in the external parts (m+3 layer) of the shell, which introduce intra-incremental heterogeneity and which cannot be reconciled with modern SST changes or SST changes recorded in the $\delta^{18}O$ values of the same shells. Our 2D approach allowed us to avoid these areas of intra-increment heterogeneity and focus on areas that are predominantly controlled by changes in SST.

These results are particularly promising for future analyses of patelloid shells for the study of season of collection in archaeological sites as well as the reconstruction of sub-annual climatic conditions in the past. Shells of the species studied here are widely available along the European Atlantic façade and the Argentinian coastline and make up a significant part of marine mollusc remains in archaeological sites of those regions (Colonese et al., 2011; Villagran et al., 2011; Zangrando et al., 2016). By using LIBS as a screening tool for targeted $\delta^{18}O$ analysis, focusing on annual minima and maxima revealed in the Mg/Ca record, researchers can improve cost and time efficiency. This novel method will enable them to increase sample numbers and produce larger, more in-depth climatic studies than previously possible.

6. Acknowledgements

Niklas Hausmann was supported by the German Research Foundation under the Emmy Noether Program (project number: 439799406). We thank the Applied Photonics Lab of the Institute of Elec- tronic Structure and Laser of the Foundation for Research and Technology - Hellas for close support with the LIBS system. We are also grateful for two anonymous reviewers who helped to improve the manuscript.

References

Bosch, M.D., Mannino, M.A., Prendergast, A.L., Wesselingh, F.P., O'Connell, T.C., Hublin, J.J., 2018. Year-round shellfish exploitation in the levant and implications for upper palaeolithic hunter-gatherer subsistence. J. Archaeol. Sci. Rep. 21, 1198–1214. doi:10.1016/j.jasrep.2017.08.014.

Colonese, A.C., Camarós, E., Verdún, E., Estévez, J., Giralt, S., Rejas, M., 2011. Integrated archaeozoological research of shell middens: New insights into hunter-gatherer-fisher coastal exploitation in tierra del fuego. The Journal of Island and Coastal Archaeology 6, 235–254. doi:10.1080/15564894.2011.586088.

Colonese, A.C., Verdún-Castelló, E., Álvarez, M., Briz i Godino, I., Zurro, D., Salvatelli, L., 2012. Oxygen isotopic composition of limpet shells from the beagle channel: implications for seasonal studies in shell middens of tierra del fuego. J. Archaeol. Sci. 39, 1738–1748. doi:10.1016/j.jas.2012.01.012.

Durham, S.R., Gillikin, D.P., Goodwin, D.H., Dietl, G.P., 2017. Rapid determination of oyster lifespans and growth rates using LA-ICP-MS line scans of shell mg/ca ratios. Palaeogeogr. Palaeoclimatol. Palaeoecol. 485, 201–209. doi:10.1016/j.palaeo.2017.06.013.

Fenger, T., Surge, D., Schöne, B., Milner, N., 2007. Sclerochronology and geochemical variation in limpet shells (patella vulgata): A new archive to reconstruct coastal sea surface temperature. Geochemistry 8. doi:10.1029/2006GC001488.

Ferguson, J.E., Henderson, G.M., Fa, D.A., Finlayson, J.C., Charnley, N.R., 2011. Increased seasonality in the western mediterranean during the last glacial from limpet shell geochemistry. Earth Planet. Sci. Lett. 308, 325–333. doi:10.1016/j.epsl.2011.05.054.

Freitas, P.S., Clarke, L.J., Kennedy, H., Richardson, C.A., 2012. The potential of combined mg/ca and 18o measurements within the shell of the bivalve pecten maximus to estimate seawater 18o composition. Chem. Geol. 291, 286–293. doi:10.1016/j.chemgeo.2011.10.023.

García-Escárzaga, A., Clarke, L.J., Gutiérrez-Zugasti, I., González-Morales, M.R., Martinez, M., López-Higuera, J.M., Cobo, A., 2018. Mg/ca profiles within archaeological mollusc (patella vulgata) shells: Laser-induced breakdown spectroscopy compared to inductively coupled plasma-optical emission spectrometry. Spectrochim. Acta Part B At. Spectrosc. 148, 8–15. doi:10.1016/j.sab.2018.05.026.

García-Escárzaga, A., Martínez-Minchero, M., Cobo, A., Gutiérrez-Zugasti, I., Arrizabalaga, A., Roberts, P., 2021. Using mg/ca ratios from the limpet patella depressa pennant, 1777 measured by laser-induced breakdown spectroscopy (LIBS) to reconstruct paleoclimate. Appl. Sci. (Basel) 11, 2959. doi:10.3390/app11072959.

García-Escárzaga, A., Moncayo, S., Gutiérrez-Zugasti, I., González-Morales, M.R., Martín-Chivelet, J., Cáceres, J.O., 2015. Mg/ca ratios measured by laser induced breakdown spectroscopy (LIBS): a new approach to decipher environmental conditions. J. Anal. At. Spectrom. 30, 1913–1919. doi:10.1039/c5ja00168d.

Giorgino, T., 2009. Computing and visualizing dynamic time warping alignments inR: ThedtwPackage. J. Stat. Softw. 31, 1–24. doi:10.18637/jss.v031.i07.

Good, S., Fiedler, E., Mao, C., Martin, M.J., Maycock, A., Reid, R., Roberts-Jones, J., Searle, T., Waters, J., While, J., Worsfold, M., 2020. The current configuration of the OSTIA system for operational production of foundation sea surface temperature and ice concentration analyses. Remote Sens. (Basel) 12, 720. doi:10.3390/rs12040720.

Graniero, L.E., Surge, D., Gillikin, D.P., Briz i Godino, I., Álvarez, M., 2017. Assessing elemental ratios as a paleotemperature proxy in the calcite shells of patelloid limpets. Palaeogeogr. Palaeoclimatol. Palaeoecol. 465, 376–385. doi:10.1016/j.palaeo.2016.10.021.

Gutiérrez-Zugasti, I., Suárez-Revilla, R., Clarke, L.J., Schöne, B.R., Bailey, G.N., González-Morales, M., 2017. Shell oxygen isotope values and sclerochronology of the limpet patella vulgata linnaeus 1758 from northern iberia: Implications for the reconstruction of past seawater temperatures. Palaeogeography, Palaeoclimatology, Palaeoecology 475, 162–175. URL: http://dx.doi.org/10.1016/j.palaeo.2017.03.018, doi:10.1016/j.palaeo.2017.03.018.

Hausmann, N., Prendergast, A.L., Lemonis, A., Zech, J., Roberts, P., Siozos, P., Anglos, D., 2019. Extensive elemental mapping unlocks mg/ca ratios as climate proxy in seasonal records of mediterranean limpets. Sci. Rep. 9, 3698. doi:10.1038/s41598-019-39959-9.

Hausmann, N., Siozos, P., Lemonis, A., Colonese, A.C., Robson, H.K., Anglos, D., 2017. Elemental mapping of mg/ca intensity ratios in marine mollusc shells using laser-induced breakdown spectroscopy. J. Anal. At. Spectrom. 32, 1467–1472. doi:10.1039/c7ja00131b.

Hausmann, N., Surge, D., Briz i Godino, I., 2024. Data and code for 'confirmation of mg/ca ratios as palaeothermometers in atlantic limpet shells'. URL: https://doi.org/10.17605/OSF.IO/JQ9MX. oSF.

Hausmann, N., Theodoraki, D., Piñon, V., Siozos, P., Lemonis, A., Anglos, D., 2023. Applying laser induced breakdown spectroscopy (LIBS) and elemental imaging on marine shells for archaeological and environmental research. Sci. Rep. 13, 19812. doi:10.1038/s41598-023-46453-w.

Inall, M., Gillibrand, P., Griffiths, C., MacDougal, N., Blackwell, K., 2009. On the oceanographic variability of the north-west european shelf to the west of scotland. J. Mar. Syst. 77, 210–226. doi:10.1016/j.jmarsys.2007.12.012.

Lazareth, C.E., Le Cornec, F., Candaudap, F., Freydier, R., 2013. Trace element heterogeneity along isochronous growth layers in bivalve shell: Consequences for environmental reconstruction. Palaeogeogr. Palaeoclimatol. Palaeoecol. 373, 39–49. doi:10.1016/j.palaeo.2011.04.024.

Martínez-Minchero, M., Cobo, A., Méndez-Vicente, A., Pisonero, J., Bordel, N., Gutiérrez-Zugasti, I., Roberts, P., Arrizabalaga, ., Valdiande, J., Mirapeix, J., López-Higuera, J.M., García-Escárzaga, A., 2023. Comparison of mg/ca concentration series from patella depressa limpet shells using CF-LIBS and LA-ICP-MS. Talanta 251, 123757. doi:10.1016/j.talanta.2022.123757.

Nicastro, A., Surge, D., Briz i Godino, I., Álvarez, M., Schöne, B.R., Bas, M., 2020. High-resolution records of growth temperature and life history of two nacella limpet species, tierra del fuego, argentina. Palaeogeogr. Palaeoclimatol. Palaeoecol. 540, 109526. doi:10.1016/j.palaeo.2019.109526.

Ortiz, J.E., Gutiérrez-Zugasti, I., Torres, T., González-Morales, M., Sánchez-Palencia, Y., 2015. Protein diagenesis in patella shells: Implications for amino acid racemisation dating. Quat. Geochronol. 27, 105–118. doi:10.1016/j.quageo.2015.02.008.

Parker, W., Yanes, Y., Mesa Hernández, E., Hernández Marrero, J.C., Pais, J., Soto Contreras, N., Surge, D., 2020. Shellfish exploitation in the western canary islands over the last two millennia. Environ. Archaeol. 25, 14–36. doi:10.1080/14614103.2018.1497821.

Poulain, C., Gillikin, D.P., Thébault, J., Munaron, J.M., Bohn, M., Robert, R., Paulet, Y.M., Lorrain, A., 2015. An evaluation of mg/ca, sr/ca, and ba/ca ratios as environmental proxies in aragonite bivalve shells. Chem. Geol. 396, 42–50. doi:10.1016/j.chemgeo.2014.12.019.

R Core Team, 2020. R core team R: a language and environment for statistical computing. Foundation for Statistical Computing .

Robson, H.K., Hausmann, N., Milner, N., 2023. Shell middens. Elsevier.

Schöne, B., Zhang, Z., Jacob, D.E., Gillikin, D., Tütken, T., Garbe-Schönberg, D., McConnaughey, T., Soldati, A., 2010. Effect of organic matrices on the determination of the trace element chemistry (mg, sr, mg/ca, sr/ca) of aragonitic bivalve shells (arctica islandica)—comparison of ICP-OES and LA-ICP-MS data. Geochemical Journal 44, 23–37. doi:10.2343/GEOCHEMJ.1.0045.

Shackleton, N.J., 1973. Oxygen isotope analysis as a means of determining season of occupation of prehistoric midden sites. Archaeometry 15, 133–141. doi:10.1111/j.1475-4754.1973.tb00082.x.

Surge, D., Barrett, J.H., 2012. Marine climatic seasonality during medieval times (10th to 12th centuries) based on isotopic records in viking age shells from orkney, scotland. Palaeogeogr. Palaeoclimatol. Palaeoecol. 350-352, 236–246. doi:10.1016/j.palaeo.2012.07.003.

Surge, D., Lohmann, K.C., 2008. Evaluating mg/ca ratios as a temperature proxy in the estuarine oyster, *Crassostrea virginica*: Mg/ca RATIOS IN OYSTER SHELLS. J. Geophys. Res. 113, G02001. doi:10.1029/2007jg000623.

Vihtakari, M., Ambrose, Jr, W.G., Renaud, P.E., Locke, V, W.L., Carroll, M.L., Berge, J., Clarke, L.J., Cottier, F., Hop, H., 2017. A key to the past? element ratios as environmental proxies in two arctic bivalves. Palaeogeogr. Palaeoclimatol.

Palaeoecol. 465, 316–332. doi:10.1016/j.palaeo.2016.10.020.
Villagran, X.S., Balbo, A.L., Madella, M., Vila, A., Estevez, J., 2011. Stratigraphic and spatial variability in shell middens: microfacies identification at the ethnohistoric site tunel VII (tierra del fuego, argentina). Archaeol. Anthropol. Sci. 3, 357–378. doi:10.1007/s12520-011-0074-z.
Wanamaker, Jr, A.D., Kreutz, K.J., Wilson, T., Borns, Jr, H.W., Introne, D.S., Feindel, S., 2008. Experimentally determined mg/ca and sr/ca ratios in juvenile bivalve calcite for mytilus edulis: implications for paleotemperature reconstructions. Geo-Mar. Lett. 28, 359–368. doi:10.1007/s00367-008-0112-8.
Wang, T., Surge, D., Mithen, S., 2012. Seasonal temperature variability of the neoglacial (3300–2500BP) and roman warm period (2500–1600BP) reconstructed from oxygen isotope ratios of limpet shells (patella vulgata), northwest scotland. Palaeogeogr. Palaeoclimatol. Palaeoecol. 317-318, 104–113. doi:10.1016/j.palaeo.2011.12.016.
Zangrando, A.F.J., Ponce, J.F., Martinoli, M.P., Montes, A., Piana, E., Vanella, F., 2016. Palaeogeographic changes drove prehistoric fishing practices in the cambaceres bay (tierra del fuego, argentina) during the middle and late holocene. Environ. Archaeol. 21, 182–192. doi:10.1080/14614103.2015.1130888.
Álvarez, M., Briz Godino, I., Balbo, A., Madella, M., 2011. Shell middens as archives of past environments, human dispersal and specialized resource management. Quat. Int. 239, 1–7. doi:10.1016/j.quaint.2010.10.025.